INTERNATIONAL JOURNAL OF MECHANICS
DOI: 10.46300/9104.2024.18.5 Volume 18, 2024

# Global Sensitivity Analysis and Surrogate Models for Evaluation of Limit States in Steel Truss Structures

Zdeněk Kala
Institute of Structural Mechanics, Faculty of Civil Engineering, Brno University of Technology,
Veveří Str. 95, Brno, ZIP 602 00,
Czech Republic

Received: June 14, 2023. Revised: August 8, 2024. Accepted: September 9, 2024. Published: October 14, 2024.

**Abstract— This article presents the global sensitivity analysis of the serviceability limit state of a steel truss using Monte Carlo simulations. The focus is on the probabilistic assessment of deflection, with failure probability defined as the likelihood of exceeding the deflection limit. Deflection is computed using the beam finite element method. A surrogate model is introduced to reduce computational costs. By integrating the surrogate and original models, significant CPU cost reductions are achieved. Furthermore, classical Sobol sensitivity analysis is used to examine the model outputs and analyze the significance of member loading and stiffness on the deflection. This study advances the use of surrogate models in global sensitivity analysis, enhancing computational efficiency and the understanding of interactions between input variables in the reliability assessment of steel truss structures.**

**Keywords— Sensitivity analysis, deflection, serviceability, limit state, structure, failure probability, surrogate modeling, structural reliability.**

## I. Introduction

Advancements in computational mechanics have significantly enhanced the field of structural mechanics, particularly in the context of stochastic analysis, [1]. The transition from purely analytical methods to computational techniques allows for a more robust and generalized approach to addressing uncertainties in structural systems. Probabilistic methods, such as Monte Carlo (MC) simulations, estimate the probability of failure or specific model outcomes. The finite element method (FEM) and MC simulations are crucial for accurately modeling the random behavior of steel structures and conducting reliability assessments, [2]. However, the integration of FEM into MC simulations is computationally demanding and requires numerous runs to estimate the failure probability. Therefore, more efficient computational strategies are necessary to manage the complexity and reduce the computational burden.

The complexity of structural mechanics models presents challenges in propagating uncertainties using classical MC approaches, necessitating many evaluations of structural responses, see, e.g., [3], [4]. Various computational models in structural mechanics offer different levels of accuracy and computational cost for estimating outputs like stress state [5], resistance [6], [7], or crack propagation [8], [9], all of which can be optimized to reduce computing costs, [10].

This article explores stochastic modeling and the use of high-fidelity and low-fidelity models to reduce computational costs while maintaining accuracy, [11]. Surrogate models enable rapid evaluations for probabilistic assessments, proving advantageous in computationally demanding global sensitivity analysis (GSA) algorithms, where failure probability estimation is repeatedly performed in nested loops. However, while the use of surrogate models significantly reduces the computational burden, challenges arise due to the lack of reliable error measures and potential inaccuracies in representing limit-state functions, especially for models with discontinuities or sharp changes in behavior, [12], [13], [14], [15].

The article aims to conduct a comprehensive GSA of failure probability $P_f$ using surrogate models and numerical simulation methods. The GSA of $P_f$ employs the Goal-Oriented Sensitivity Analysis approach with contrast functions, [16]. Previous studies [17], [18] explored the GSA of $P_f$, and [16] presented a generalized framework for sensitivity indices, linking them with Sobol sensitivity analysis, [19], [20]. This article uses the GSA of $P_f$ based on entropy [21] as an alternative to [16].

Research on surrogate models has advanced [14], but not all

models suit every GSA. Fundamental surrogate models include Response Surface Methodology [22], Kriging [23], Support Vector Regression [24] and Artificial Neural Networks [25]. Surrogate model applications are well-documented, [26], [27], [28], [29], [30].

The aim of this study is to bridge the gap between computational efficiency and accuracy in reliability assessments of steel truss structures. By leveraging both high-fidelity and low-fidelity models, the optimization of global sensitivity analysis methods and improvement in failure probability estimation are sought. The integration of surrogate models offers a promising solution to the computational demands specific to steel truss structures. In the next section, the specifics of reliability-oriented global sensitivity analysis, its methodologies, and applications in structural mechanics will be explored.

## II. Reliability-oriented Global Sensitivity Analysis

GSA methods identify the influence of individual input variables on system output values and highlight their importance in models and simulations, [31]. Consider a limit state function with random variables $R$ (resistance) and $A$ (load action):

$$Z = R - A. \tag{1}$$

Reliability analysis relies on probabilistic analysis, focusing on the frequency of failures $Z<0$. The probability of failure $P_f$ is given as:

$$P_f = E(1_{Z<0}). \tag{2}$$

Reliability-oriented GSA includes sensitivity measures reflecting the contribution of individual input variables to $P_f$ variability, [21]. Sensitivity measures based on variance and entropy, effective in $P_f$ analysis [21], are used here. Sobol sensitivity analysis [19], [20] also assesses the contribution of individual variables to the total output variance V(Z). Variance-based GSA is derived from Sobol's GSA, where the variance of the binary function $1_{Z<0}$ is used instead of the model output $R$, $A$ or $Z$.

$$V(1_{Z<0}) = P_f \cdot (1 - P_f). \tag{3}$$

This measure, introduced in [17] and [18], is part of the contrast-based sensitivity measures described in [16]. The second measure uses entropy:

$$H(1_{Z<0}) = -P_f \cdot \ln(P_f) - (1 - P_f) \cdot \ln(1 - P_f). \tag{4}$$

Both measures indicate the degree of uncertainty in relation to $P_f$. The dome-shaped entropy function in Equation (4) approximates the dome-shaped variance function described in Equation (3).

Variance and entropy measures provide insights into input variables' influence on $P_f$. However, these measures may not be directly comparable. Sensitivity indices derived from the decomposition of the total uncertainty in $P_f$ offer a comparative overview of variable importance, [21]. The first-order reliability-oriented sensitivity index based on sensitivity measure $SM(P_f)=\{V(1_{Z<0}), H(1_{Z<0})\}$ is:

$$S_i = \frac{SM(P_f) - E(SM(P_f|X_i))}{SM(P_f)}. \tag{5}$$

The second-order reliability-oriented sensitivity index is:

$$S_{ij} = \frac{SM(P_f) - E(SM(P_f|X_i, X_j))}{SM(P_f)} - S_i - S_j. \tag{6}$$

The third-order reliability-oriented sensitivity index is:

$$S_{ijk} = \frac{SM(P_f) - E(SM(P_f|X_i, X_j, X_k))}{SM(P_f)} - S_i - S_j - S_k - S_{ij} - S_{ik} - S_{jk}. \tag{7}$$

Higher-order sensitivity indices reveal interactions and non-linear effects between variables, providing a comprehensive understanding of each variable's relative importance on $Z$ or $P_f$. These indices ensure the sum of all sensitivity indices equals one, reflecting the total contribution of input variables to reliability output.

$$\sum_i C_i + \sum_i \sum_{j>i} C_{ij} + \sum_i \sum_{j>i} \sum_{k>j} C_{ijk} + \ldots + C_{123..M} = 1. \tag{8}$$

This concept of sensitivity analysis ensures a thorough assessment of the overall variability or uncertainty of reliability. The results of GSA enhance the understanding of interactions among input variables and non-linear effects influencing structural reliability. This allows for more informed decision-making based on the probability of failure, [32], [33], [34], [35].

## III. Engineering Case Study

This study focuses on a steel truss structure. The members are seamless steel tubes with an outer diameter of 88.9 mm, per EN 10255. The top chord uses CHS 88.9 x 10 circular hollow profiles, and other members use CHS 88.9 x 8. The wall thicknesses are 10 mm for the top chord and 8 mm for the others. The material is steel grade 355 MPa.

### *A. The Finite Element Model*

The main outputs are midspan deflection $w$ and horizontal deflection $\Delta$. These deflections are computed using the beam finite element method. Deformation depends linearly on the load, assuming geometric and material linearity. The model is symmetric in geometry, material, and load. Thus, $w$ and $\Delta$ can be computed using left-right symmetry, simplifying the model to half of the truss (Fig. 1).

Steel grade S355 is used for all members. Dimensioning of cross-sections is based on the assumption that the three bars in the top chord are under compression and the two bars in the bottom chord are in tension (Fig. 1). The maximum axial tensile stress of 354.7 MPa, which is close to the yield strength of 355 MPa, occurs in bar five. Thus, 128 kN is the design

load-carrying capacity per Eurocode 3, [36], (EC3) and EN 1990 [37] standards.

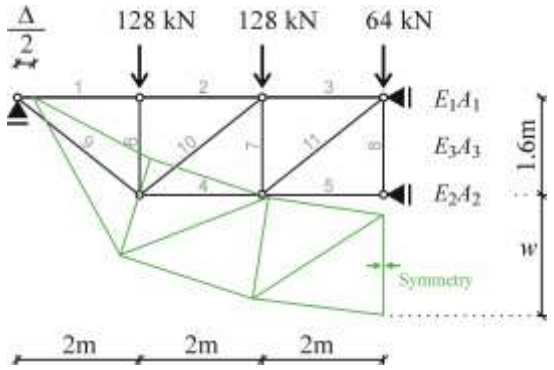


Fig. 1 Beam computational model of steel truss structure.

Truss deformations are random outputs of the stochastic model, depending on the variability of load and stiffness. Statistical characteristics of load and material parameters are derived from experimental research [38] and design values from standards, [36], [37]. The $R_k$=128 kN design load includes a permanent load action of 28 kN and a variable load action of 100 kN. According to [36], the design load action is:

$$\frac{R_k}{\gamma_M} = \gamma_G \cdot G_k + \gamma_Q \cdot Q_k, \tag{9}$$

where $\gamma_M$=1.0 is the material partial safety factor and $\gamma_G$=1.35 and $\gamma_Q$=1.5 are the partial safety factors for characteristic permanent load action $G_k$ and characteristic long-term variable load action $Q_k$ [37], [39]. The characteristic values calculated according to the static model in [37], [39] are $G_k$=20.74 kN and $Q_k$=66.67 kN.

### B. The input random quantities

The statistical characteristics of permanent and characteristic load actions can be derived from the concept described in [37], [39]. The permanent load follows a Gaussian distribution with a mean $G_k$ and a coefficient of variation of 0.1, [40]. The variable load follows a Gumbel-max distribution with a mean of $0.6 \cdot Q_k$ and a standard deviation of $0.21 \cdot Q_k$ [37], [39], (Table I).

Cross-sectional stiffnesses are additional input random variables, represented by the product of the cross-sectional area $A$ and Young's modulus $E$. The top bars have $A_1$ and $E_1$, bottom bars $A_2$ and $E_2$, and diagonal/vertical bars $A_3$ and $E_3$, (Fig. 1). Young's modulus $E$ has a mean of 210 GPa and a standard deviation of 10 GPa, [41]. Statistical characteristics of A are derived from experimental research [38]: $\mu_{A1}$=2480 mm$^2$, $\sigma_{A1}$=155 mm$^2$, $\mu_{A2}=\mu_{A3}$=2030 mm$^2$, and $\sigma_{A2}=\sigma_{A3}$=127 mm$^2$. The lengths of the bars are considered to be deterministic values without any variability.

To simplify the stochastic analysis, $A$ and $E$ are replaced by a single random variable $k=E \cdot A$. This reduction in dimensionality allows all variables to be considered with the same unit, Newton, making the study more transparent. This dimensional reduction is valid because $A$ and $E$ always appear as a product. The mean $\mu_k$, standard deviation $\sigma_k$, and skewness $a_k$ of $k$ are calculated as:

$$\mu_k = \mu_E \cdot \mu_A \cdot \tag{10}$$

$$\sigma_k = \sqrt{\mu_E^2\sigma_A^2 + \sigma_E^2\mu_A^2 + \sigma_E^2\sigma_A^2}\ . \tag{11}$$

$$a_k = 6\frac{\mu_{EA}}{\sigma_{EA}^3}\sigma_E^2\sigma_A^2 \cdot \tag{12}$$

The product of the cross-sectional area and Young's modulus can be accurately approximated using a three-parameter lognormal distribution, as demonstrated in [39]. All input variables, $\boldsymbol{X}=\{G, Q, k_1, k_2, k_3\}$, are listed in Table I.

TABLE I. INPUT RANDOM QUANTITIES

| Symbol | Density | Mean value | St. deviation | St. skewness |
|---|---|---|---|---|
| $k_1$ | Lognormal | 520.8 MN | 40.95 MN | 0.11 |
| $k_2$ | Lognormal | 426.3 MN | 33.54 MN | 0.11 |
| $k_3$ | Lognormal | 426.3 MN | 33.54 MN | 0.11 |
| $G$ | Gauss | 28 kN | 2.8 kN | 0 |
| $Q$ | Gumbel-max | 60 kN | 21 kN | 1.14 |

### C. The input random quantities

The reliability condition requires that the midspan deflection $w$ must be less than or equal to 1/250 of the span, where the tolerance limit of 1/250 is mentioned in EC3. For a truss with a span of 12 m, the deflection $w$ must not exceed 48 mm. Failure occurs if the deflection $w$ is higher than 48 mm. The failure probability is analyzed using a binary random variable $1_{w\geq 48mm}$, (Fig. 2).

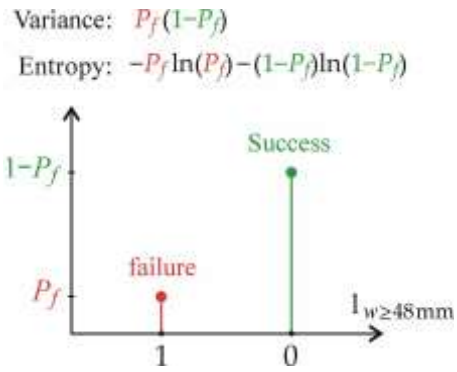


Fig. 2 The Bernoulli trial of failure (1) vs success (0).

The failure probability can be computed as the mean value from the binary random variable $1_{w\geq 48mm}$.

$$P_f = E\left(1_{w\geq 48\,\mathrm{mm}}\right). \tag{13}$$

The midspan deflection $w(\boldsymbol{X})$ is computed using the beam finite element method for the input random vector of the FE model, $\boldsymbol{X}$, which consists of the five random variables listed in Table I. The statistical analysis of the midspan deflection based on the FE model is shown in Fig. 3.

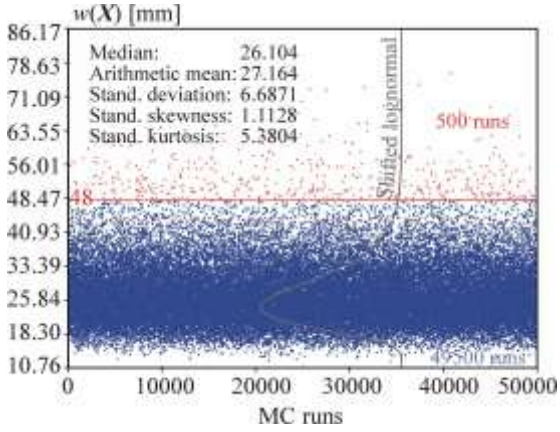


Fig. 3 Steel truss structure computational model.

The distribution of the random realizations of $w$ can be successfully approximated using a three-parameter lognormal pdf. In each MC run, the output is a failure (1) or success (0). Random realizations representing failure are deflections higher than 48 mm. Such deflections are less frequent and are located in the probability distribution at the tail of the pdf, see the red realizations in Fig. 3. The failure probability is defined as the probability $P_f = \mathrm{P}[w(\boldsymbol{X}) \geq 48 \text{ mm}]$. The MC method can be used to calculate the failure probability as:

$$P_f \approx \frac{1}{K} \sum_{k=1}^{K} 1_{w(x_k) \geq 48\,\mathrm{mm}} . \tag{14}$$

The failure probability $P_f$ is computed using $K$=50 000 runs of the MC method with the inputs from Table I. The numerical estimate obtained in this manner is $P_f = 0.01$.

### D. Surrogate model

Sensitivity analysis in structural engineering often requires extensive computational resources, especially with Monte Carlo simulations. Implementing surrogate models reduces the computational load while maintaining accuracy in estimating failure probabilities $P_f$.

Estimating $P_f$ in the previous chapter required numerous MC simulations for accuracy. GSA based solely on the FEM model would be very demanding for repeated estimations of $P_f$. A higher number of MC runs is necessary for GSA compared to a single $P_f$ estimate. To address this, a surrogate model is implemented to speed up $P_f$ estimation while preserving accuracy. This involves quickly identifying runs where deflection $w$ is reliably below the limit value, thus avoiding detailed FEM calculations. The FEM is used only for deformations exceeding the limit value (failure) or near the boundary between failure and success. Smaller deformations are calculated using the surrogate model. For rare failures, a more accurate FE model is used with less CPU load in all simulations, making the surrogate model useful for estimating global sensitivity indices by enabling numerous simulation runs.

The output of the FE model presented here is the midspan deflection $w$. This deflection can be approximated by the following function:

$$\tilde{w}(X) = F \cdot \left( \frac{c_1}{k_1} + \frac{c_2}{k_2} + \frac{c_3}{k_3} \right). \tag{15}$$

In Equation (15), the approximated deformation is directly proportional to the load $F$ and inversely proportional to the stiffnesses of the bars $k_1$, $k_2$, and $k_3$, see Table I. Parameters $c_1$, $c_2$, and $c_3$ are computed for unit load $F$ =1 using $k_{01}$ = 210 GPa · 2480 mm$^2$ = 520.8 MN and $k_{02} = k_{03}$ = 210 GPa · 2030 mm$^2$ = 426.3 MN, where $k_{01}$, $k_{02}$, and $k_{03}$ are the median of the cross-sectional stiffnesses, which are calculated using the medians of $E$ and $A$. The parameters $c_1$, $c_2$, and $c_3$ are approximately estimated in the area of failure when the deflection exceeds 48 mm, which occurs when the stiffnesses of the bars $k_{01}$, $k_{02}$, and $k_{03}$ are reduced by a coefficient of approximately 0.83. Parameters $c_1$, $c_2$, and $c_3$ can be calculated from a system of three linear equations using permutation without repetition from the set {0.82, 0.83, 0.84}. Three of the six permutations are chosen such that each parameter $c_1$, $c_2$, and $c_3$ is divided by a different stiffness in each equation, see Equation (16), Equation (17), and Equation (18).

$$1 \cdot \left( \frac{c_1}{0.82 \cdot 520.8 \cdot 10^6} + \frac{c_2}{0.83 \cdot 426.3 \cdot 10^6} + \frac{c_3}{0.84 \cdot 426.3 \cdot 10^6} \right) = w_{FEM1} \tag{16}$$

$$1 \cdot \left( \frac{c_1}{0.83 \cdot 520.8 \cdot 10^6} + \frac{c_2}{0.84 \cdot 426.3 \cdot 10^6} + \frac{c_3}{0.82 \cdot 426.3 \cdot 10^6} \right) = w_{FEM2} \tag{17}$$

$$1 \cdot \left( \frac{c_1}{0.84 \cdot 520.8 \cdot 10^6} + \frac{c_2}{0.82 \cdot 426.3 \cdot 10^6} + \frac{c_3}{0.83 \cdot 426.3 \cdot 10^6} \right) = w_{FEM3} \tag{18}$$

The right-hand sides are the midspan deformations calculated using FEM. The matrix of the system of three equations is symmetric, and its determinant is positive. The values of parameters $c_1$ = 40.562, $c_2$ = 67.178, and $c_3$ = 30.397 are obtained by solving this system of equations. The final surrogate model for load action $F = G + Q$ can be expressed as:

$$\tilde{w}(X) = F \cdot \left( \frac{40.5619}{k_1} + \frac{67.1778}{k_2} + \frac{30.3974}{k_3} \right). \tag{19}$$

In Equation (19), the input random variables $G$, $Q$, $k_1$, $k_2$, and $k_3$ are introduced in base units of Newton, and the output deflection is in meters. The statistical characteristics of the input random variables for which the surrogate model is created are defined in Table I and need to be converted to base units before being used in Equation (19).

### E. The function of serviceability limit state

In structural engineering, ensuring reliability in design involves verifying that deflections remain within acceptable limits. For this study, the design is considered reliable if the midspan deflection $w$ is less than 0.048 m. By combining the

finite element method (FEM) and surrogate models, the serviceability limit state can be effectively evaluated, optimizing computational efficiency while maintaining accuracy.

$$g(\boldsymbol{X}) = \begin{cases} 0.48 - w(\boldsymbol{X}), & \text{for } 1.01 \cdot \tilde{w}(\boldsymbol{X}) > 0.048 \text{ m} \\ 0.48 - \tilde{w}(\boldsymbol{X}), & \text{for } 1.01 \cdot \tilde{w}(\boldsymbol{X}) \le 0.048 \text{ m} \end{cases}. \quad (20)$$

The parameter 1.01 introduced in Equation (20) is numerically (heuristically) set so that the FEM is used for all points of the input space in the failure region, especially near the failure-success boundary.

Fig. 4 shows the grey area that forms the boundary between the region of failure and success. Failure occurs near zero, which is highlighted in red behind the area. Approaching zero means less stiffness and, thus, more deflection.

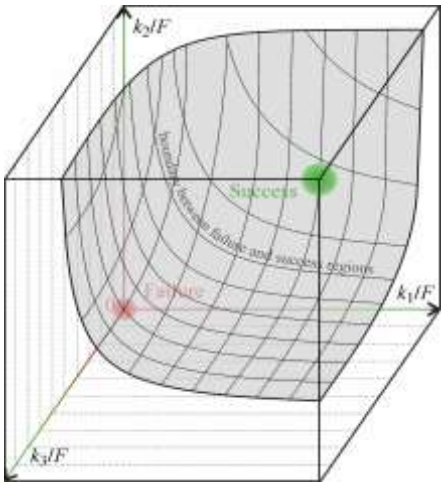


Fig. 4 The boundary between the region of failure and success.

The occurrence of failure is rare; thus, most runs do not need to be evaluated using the FEM. The closer we are to the green point in Fig. 4, the less we need the FE model. The accuracy of the surrogate model was numerically verified using 50,000 LHS runs across the spectrum of random realizations, (Fig. 5).

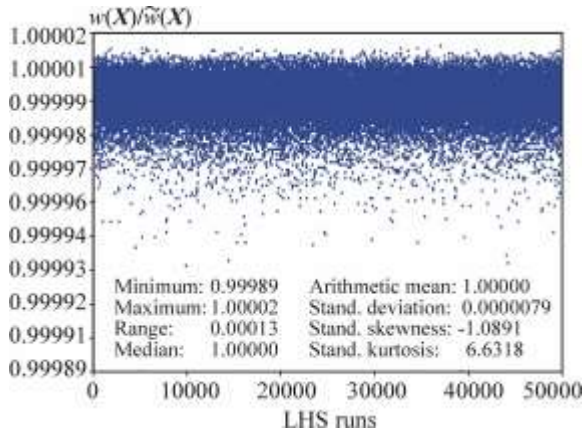


Fig. 5 Comparison of the FEM and surrogate model.

It can be observed that the deviations of the surrogate model from the FE model are minimal, (Fig. 5). The parameter 1.01 was heuristically set and may vary depending on the type of the surrogate model.

### *F. The global sensitivity analysis results*

Understanding the impact of input variables on the reliability of structural designs is crucial for effective engineering decisions. GSA provides a comprehensive method to assess how different input variables influence the failure probability of $P_f$ and other model outputs.

GSA of $P_f$ is based on the variance decomposition of the Bernoulli distribution $V(1_{w \ge 48}) = P_f \cdot (1\text{-}P_f)$, [17], [18].

The numerical estimation of the sensitivity index $S_i$ in Equation (5) is performed using the double-nested-loop algorithm. Using LHS runs, the outer loop is repeated 5000 times to estimate the arithmetic mean $E(\cdot)$ of the samples. The inter-loop result is the estimate of the conditional $P_f$. In the inner loop, each sample $SM(P_f)$ has the estimation of $P_f$ realized using 20 million runs. Although a large number of runs have been used and MC could have been employed, the Latin Hypercube Sampling (LHS) [42], [43] method is preferred due to the slightly better results in the double-loop simulations. The calculation of the sensitivity index $S_{ij}$ from Equation (6) and other indices is performed analogously. The conditional estimates of $P_f$ are extremely computationally demanding, so they were treated using the surrogate model in Equation (19).

Fig. 6 shows the results of the GSA of $P_f$ based on the sensitivity measure from Equation (3). Fig. 7 shows the results of the GSA of $P_f$ based on the sensitivity measure from Equation (4). In both cases, the variation load action $Q$ has a dominant influence on $P_f$, (Table I). The second significant effect is the interaction effect between $Q$ and the stiffness of the bottom chord $k_2$. However, this is a minor effect in comparison to the first-order effect due to $Q$. On the contrary, the influences of $G$, $k_1$, $k_2$, and $k_3$ on $P_f$ are negligible in both main and interaction effects.

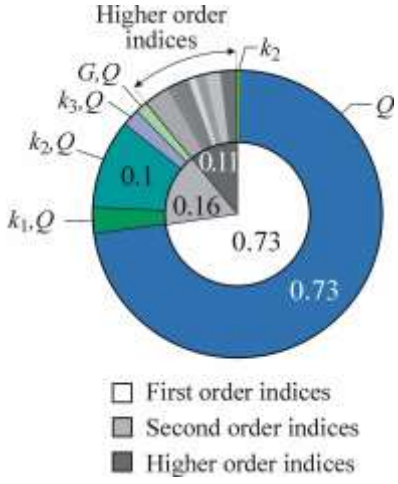


Fig. 6 The results of GSA based on the contrast sensitivity measure from Equation (3).

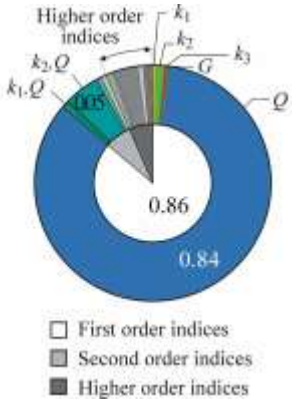


Fig. 7 The results of GSA based on the entropy sensitivity measure from Equation (4).

The computational speed was measured on a single-core CPU Intel Core i7-3740QM with a processor frequency from 2.70 GHz to 3.70 GHz (boost). The estimated time required to calculate one index using the surrogate model is approximately one hour, whereas using the original FE model would take about 40 hours. By comparing these two measures, it can be stated that the surrogate model accelerates the estimation of sensitivity indices approximately forty times. The time consumption is the same when using Equation (3) or Equation (4). The calculation of all 32 indices would be 32 times more demanding, but the estimation of each index could be performed parallelly. This would make it possible to run the calculation of individual indices in parallel. Multiple cores or processors could be used to compute multiple indices simultaneously. This would significantly speed up the overall calculation of all indices.

The classical Sobol SA is added for comparison. Sobol SA analyses the influence of input random variables on the model output rather than specifically focusing on $P_f$. The midspan deflection $w$ is considered as the model output. Sobol SA analyses the influence of input variables $k_1$, $k_2$, $k_3$, $G$, and $Q$ (model inputs) on the midspan deflection $w$. The calculation is based on the double-nested-loop algorithm. Using the LHS runs, the outer loop is repeated 5000 times to estimate the arithmetic mean $E(\cdot)$ of the variance samples $V(w|X_i)$. Each sample $V(w|X_i)$ is estimated by the inner loop algorithm using 5000 samples. Random sampling was generated using the LHS method.

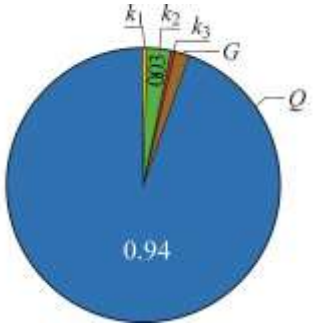


Fig. 8 The results of Sobol SA using random quantities $k_1$, $k_2$, $k_3$, $G$, $Q_2$.

By including all five input random variables in Sobol sensitivity analysis, the dominant influence of the input variable $Q$ was confirmed, (Fig. 8). The numerical estimates of the sensitivity indices in Fig. 8 are $S_1$= 0.007 ($k_1$), $S_2$= 0.027 ($k_2$), $S_3$= 0.006 ($k_3$), $S_4$= 0.017 ($G$), with dominant influence of $S_5$=0.943 ($Q$). Although Fig. 8 offers an insight into the influence of all input variables, the influence of stiffnesses $k_1$, $k_2$, and $k_3$ is overshadowed by the dominant influence of $Q$. Therefore, the results are supplemented by another study, where the loads $G$ and $Q$ are introduced as deterministic quantities, (Fig. 9).

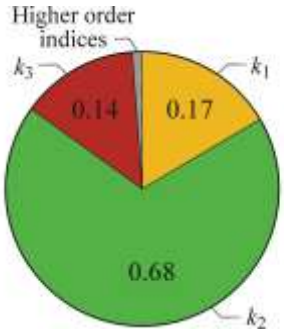


Fig. 9 The result of Sobol SA using only random quantities $k_1$, $k_2$ and $k_3$.

The results shown in Fig. 9 show that the variability of the cross-sectional stiffness of the bottom chord $k_2$ has a dominant effect on the midspan deflection $w$. The stiffnesses $k_1$ and $k_3$ have approximately the same influence, which is small but may be important in the sum. In terms of influence on the midspan deflection $w$, the stiffnesses of the diagonal and vertical members $k_3$ are as significant as the stiffness of the top chord. Fig. 9 shows that higher-order interaction effects are minimal, which is the usual result of Sobol sensitivity analysis of model outputs in structural mechanics, [44].

The top bars are under compression and dimensioned to take into account buckling. Although the top bars have a larger area than the other bars, the variation coefficients of all stiffnesses $k_1$, $k_2$ and $k_3$ are the same. The Sobol sensitivity analysis presented here shows that the influence of the stiffnesses of the diagonal and vertical members can be comparable to those of the top chord members.

The sensitivity indices shown in Fig. 6 and Fig. 7 can be converted into total indices, which is shown in Fig. 10. The total index $S_{Ti}$ offers a more transparent understanding of the influence of $X_i$, taking into account all potential interaction effects between $X_i$ and the remaining variables. Therefore, the total index is highly valued for a comprehensive comparison of the influence of all input variables, especially when multiple input variables influence the observed output, [31]. The total sensitivity indices oriented to reliability-based sensitivity measure SM($P_f$) are derived from Sobol's method and are defined and explained in [21]. Fig. 10 shows two types of total sensitivity indices. "Contrast" refers to the total sensitivity indices computed using Equation (3), while "Entropy" denotes the total sensitivity indices computed using Equation (4).

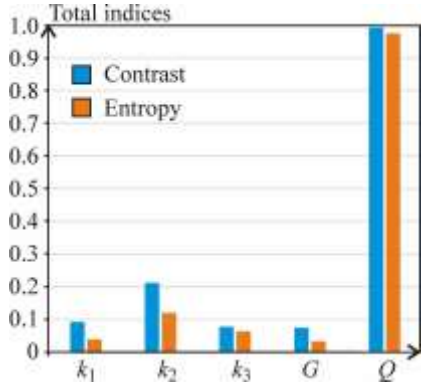


Fig. 10 The result of Sobol SA using only random quantities $k_1$, $k_2$ and $k_3$.

The sensitivity analysis results in Fig. 10, which present the total indices, answer the question of which input random variables can be neglected to simplify the stochastic computational model. Based on the above-mentioned results, input random variables $k_1$, $k_2$ or $G$, $k_1$, $k_2$ can be neglected, (Fig. 10). On the contrary, it can be recommended to model the input random variable $Q$ as accurately as possible, as its variability significantly influences the deflection.

## IV. Conclusion

A surrogate model was developed to calculate deflection in a truss structure and integrated with an original finite element model in the presented study. This surrogate, especially near the failure boundary, captured subtle changes in failure probability due to fixed input variables or their combinations. The surrogate model proved essential for real-time sensitivity analysis, significantly reducing computational time compared to the iterative runs of the original model. It was effectively applied in the global sensitivity analysis (GSA), with a focus on the reliability assessment of the steel truss's serviceability limit state, where failure is defined as excessive deflection.

The GSA revealed that failure probability is highly sensitive to variations in long-term variable load action, showing significant random variability, while the dead load had a negligible effect. The study also identified significant and less significant members based on stiffness, with the variability of stiffness in lower members substantially affecting failure probability. Classical Sobol sensitivity analysis validated these results, indicating that deflection is primarily influenced by load action variations. Another variant of GSA isolated bar stiffness effects, showing that bottom chord stiffness had the most significant impact on deflection, with the top chord, diagonal, and vertical members showing a smaller but notable influence.

Integration of surrogate models with GSA methods proved effective in structural reliability assessment, significantly reducing the time required to estimate sensitivity indices. The study highlights the potential for further development of surrogate models to optimize stochastic computational models in reliability and sensitivity analysis. The results of the GSA identified influential input variables that should be prioritized when determining their statistical characteristics, even at the expense of less influential input variables. Refining the statistical characteristics of these influential variables will improve the accuracy of probabilistic reliability analysis and enhance the understanding of structural reliability under probabilistic conditions.

## Acknowledgment

The work has been supported and prepared within the project "Importance of Stochastic Interactions in Computational Models of Structural Mechanics" of The Czech Science Foundation (GACR, https://gacr.cz/) no. 23-04712S, Czechia.

## Declaration of Generative AI and AI-assisted Technologies in the Writing Process

During the preparation of this work, the author used Grammarly for language editing. After using this service, the author reviewed and edited the content as needed and took full responsibility for the content of the publication.

## References

[1] R.E. Melchers, A.T. Beck, *Structural Reliability Analysis and Prediction*, John Wiley & Sons, 2017. https://doi.org/10.1002/9781119266105.

[2] G. Stefanou, "The stochastic finite element method: Past, present and future," *Computer Methods in Applied Mechanics and Engineering*, vol. 198, pp. 1031–1051, 2009. https://doi.org/10.1016/j.cma.2008.11.007.

[3] E. Acar, G. Bayrak, Y. Jung, I. Lee, P. Ramu, S.S. Ravichandran, "Modeling, analysis, and optimization under uncertainties: a review," *Structural and Multidisciplinary Optimization*, vol. 64, pp. 2909–2945, 2021. https://doi.org/10.1007/s00158-021-03026-7.

[4] I. Doltsinis, "Stochastic aspects of the plastic limit," *WSEAS Transactions on Applied and Theoretical Mechanics*, vol. 14, pp. 28–40, 2019.

[5] R. Grzejda, "Modeling the normal contact characteristics between components joined in multi-bolted systems," *WSEAS Transactions on Applied and Theoretical Mechanics*, vol. 19, pp. 73–81, 2024. https://doi.org/10.37394/232011.2024.19.8.

[6] L. Puklický, "The use of stainless steel in structures: Columns under compression," *IOP Conference Series: Materials Science and Engineering*, vol. 960, 032073, 2020. https://doi.org/10.1088/1757-899X/960/3/032073

[7] A. Omishore, "Uncertainty analysis of the cross-sectional area of a structural member," in *Proc. of the 4th WSEAS Int. Conf. on EMESEG'11*, Corfu, 2011, pp. 284–288.

[8] V. Kozák and J. Vala, "Modelling of crack formation and growth using FEM for selected structural materials at static loading," *WSEAS Transactions on Applied and Theoretical Mechanics*, vol. 18, pp. 243–254, 2023. https://doi.org/10.37394/232011.2023.18.23.

[9] J.M. Dias, "Damage of infill masonry walls due to vertical loads in buildings with reinforced concrete

structure," *WSEAS Transactions on Applied and Theoretical Mechanics*, vol. 18, pp. 32–49, 2023. https://doi.org/10.37394/232011.2023.18.4.

[10] I. Negrin, M. Kripka, V. Yepes, "Metamodel-assisted design optimization in the field of structural engineering: A literature review," *Structures*, vol. 52, 609–631, 2023. https://doi.org/10.1016/j.istruc.2023.04.006.

[11] B. Peherstorfer, K. Willcox, M. Gunzburger, "Survey of multifidelity methods in uncertainty propagation, Inference, and optimization," *SIAM Review*, vol. 60, no. 3, pp. 550–591, 2018. https://doi.org/10.1137/16M1082469.

[12] V. Dubourg, B. Sudret, "Meta-model-based importance sampling for reliability sensitivity analysis," *Structural Safety*, vol. 49, pp. 27–36, 2014. https://doi.org/10.1016/j.strusafe.2013.08.010.

[13] F.A. Lucay, "Accelerating global sensitivity analysis via supervised machine learning tools: Case studies for mineral processing models," *Minerals*, vol. 12, 750, 2022. https://doi.org/10.3390/min12060750.

[14] N. Tsokanas, R. Pastorino, B. Stojadinović, "A Comparison of surrogate modeling techniques for global sensitivity analysis in hybrid simulation," *Machine Learning and Knowledge Extraction*, vol. 4, pp. 1–21, 2022. https://doi.org/10.3390/make4010001.

[15] C. Boursier Niutta, E.J. Wehrle, F. Duddeck, G. Belingardi, "Surrogate modeling in design optimization of structures with discontinuous responses: A new approach for ill-posed problems in crashworthiness design," *Structural and Multidisciplinary Optimization*, vol. 57, pp. 1857–1869, 2018. https://doi.org/10.1007/s00158-018-1958-7.

[16] J.C. Fort, T. Klein, N. Rachdi, "New sensitivity analysis subordinated to a contrast," *Communications in Statistics - Theory and Methods*, vol. 45, no. 15, pp. 4349–4363, 2016. https://doi.org/10.1080/03610926.2014.901369

[17] L. Li, Z. Lu, J. Feng, B. Wang, "Moment-independent importance measure of basic variable and its state dependent parameter solution," *Structural Safety*, vol. 38, pp. 40–47. https://doi.org/10.1016/j.strusafe.2012.04.001.

[18] P. Wei, Z. Lu, W. Hao, J. Feng, B. Wang, "Efficient sampling methods for global reliability sensitivity analysis," *Computer Physics Communications*, vol. 183, no. 8, pp. 1728–1743. https://doi.org/10.1016/j.cpc.2012.03.014.

[19] I. M. Sobol, "Sensitivity estimates for nonlinear mathematical models," *Mathematical Modelling and Computational Experiments*, vol. 1, no. 4, pp. 407–414, 1993.

[20] I. M. Sobol, "Global sensitivity indices for nonlinear mathematical models and their Monte Carlo estimates," *Mathematics and Computers in Simulation*, vol. 55, no. 1-3 pp. 271–280, 2001. https://doi.org/10.1016/S0378-4754(00)00270-6.

[21] Z. Kala, "New importance measures based on failure probability in global sensitivity analysis of reliability," *Mathematics*, vol. 9, no. 19, 2425, 2021. https://doi.org/10.3390/math9192425.

[22] G.E.P. Box, K.B. Wilson, "On the experimental attainment of optimum conditions," *Journal of the Royal Statistical Society: Series B (Methodological)*, vol. 13, no. 1, pp.1–38, 1951. https://doi.org/10.1111/j.2517-6161.1951.tb00067.x.

[23] J. Sacks, W.J. Welch, T.J. Mitchell, H.P. Wynn, "Design and analysis of computer experiments," *Statistical Science*, vol. 4, no. 4, pp. 409–423, 1989. https://doi.org/10.1214/ss/1177012413.

[24] A.J. Smola, B. Schölkopf, "A tutorial on support vector regression," *Statistics and Computing*, vol. 14, no. 3, pp. 199–222, 2004. https://doi.org/10.1023/B:STCO.0000035301.49549.88.

[25] E. Másson, Y.-J. Wang, "Introduction to computation and learning in artificial neural networks," *European Journal of Operational Research*, vol. 47, no. 1, pp. 1–28, 1990. https://doi.org/10.1016/0377-2217(90)90085-P.

[26] A. Manik, K. Gopalakrishnan, A. Singh, S. Yan, "Neural networks surrogate models for simulating payment risk in pavement construction," *Journal of Civil Engineering and Management*, vol 14, no. 4, pp. 235–240, 2008. https://doi.org/10.3846/1392-3730.2008.14.22.

[27] D. Lehký, M. Šomodíková, "Reliability analysis of post-tensioned bridge using artificial neural network-based surrogate model," *Communications in Computer and Information Science*, vol. 517, 35–44, 2015. https://doi.org/10.1007/978-3-319-23983-5_4.

[28] K. Cheng, Z. Lu, C. Ling, S. Zhou, "Surrogate-assisted global sensitivity analysis: An overview," *Structural and Multidisciplinary Optimization*, vol. 61, pp. 1187–1213, 2020. https://doi.org/10.1007/s00158-019-02413-5.

[29] L. Pan, L. Novák, D. Lehký, D. Novák, M. Cao, "Neural network ensemble-based sensitivity analysis in structural engineering: Comparison of selected methods and the influence of statistical correlation," *Computer & Structures*, vol. 242, 106376, 2021. https://doi.org/10.1016/j.compstruc.2020.106376.

[30] J. Kudela, R. Matousek, "Recent advances and applications of surrogate models for finite element method computations: a review," *Soft Computing*, vol. 26, no. 24, pp. 13709–13733, 2022. https://doi.org/10.1007/s00500-022-07362-8.

[31] A. Saltelli, M. Ratto, T. Andres, F. Campolongo, J. Cariboni, D. Gatelli, M. Saisana, S: Tarantola, *Global Sensitivity Analysis*, John Wiley & Sons, Ltd., 2008. https://doi.org/10.1002/9780470725184.

[32] I. J. Navarro, J. V. Martí, V. Yepes, "Reliability-based maintenance optimization of corrosion preventive designs under a life cycle perspective," *Environmental Impact Assessment Review*, vol. 74, pp. 23–24, 2019. https://doi.org/10.1016/j.eiar.2018.10.001.

[33] A. Čereška, A. Podviezko, E. K. Zavadskas, "Assessment of different metal screw joint parameters by using multiple criteria analysis methods," *Metals*, vol. 8, 318, 2018. https://doi.org/10.3390/met8050318.

[34] E. K. Zavadskas, E. R. Vaidogas, "Multiattribute selection from alternative designs of infrastructure components for accidental situations," *Computer-Aided Civil and Infrastructure Engineering*, vol. 24, no. 5, pp. 346–358, 2009. https://doi.org/10.1111/j.1467-8667.2009.00593.x.

[35] E. R. Vaidogas, E. K. Zavadskas, "Introducing reliability measures into multi-criteria decision-making," *International Journal of Management and Decision Making*, vol. 8, no. 5–6, pp. 475–496, 2007. https://doi.org/10.1504/IJMDM.2007.013413.

[36] EN 1993-1-1:2005, Eurocode 3 — Design of steel structures - Part 1-1: General rules and rules for buildings, CEN, Brussels 2005.

[37] EN 1990: Eurocode - Basis of structural design, CEN 2002, Brussels.

[38] J. Melcher, Z. Kala, M. Holický, M. Fajkus, L. Rozlívka, "Design Characteristics of Structural Steels Based on Statistical Analysis of Metallurgical Products," *Journal of Constructional Steel Research*, vol. 60, no. 3-5, pp. 795–808. https://doi.org/10.1016/S0143-974X(03)00144-5.

[39] Z. Kala, "Limit states of structures and global sensitivity analysis based on Cramér-von mises distance," *International Journal of Mechanics*, vol. 14, pp. 107–118, 2020. https://doi.org/10.46300/9104.2020.14.14.

[40] D. Honfi, A. Mårtensson, A. S. Thelandersson, "Reliability of beams according to Eurocodes in serviceability limit state," *Engineering Structures* vol. 35, pp. 48–54, 2012. https://doi.org/10.1016/j.engstruct.2011.11.003.

[41] G.C. Soares, "Uncertainty modelling in plate buckling," *Structural Safety*, vol. 5, pp. 17–34, 1988. https://doi.org/10.1016/0167-4730(88)90003-3.

[42] M.D. McKey, R.J. Beckman, W.J. Conover "A comparison of the three methods of selecting values of input variables in the analysis of output from a computer code," *Technometrics*, vol. 21, pp. 239–245, 1979. https://doi.org/10.2307/1268522.

[43] R.C. Iman, W.J. Conover, "Small sample sensitivity analysis techniques for computer models with an application to risk assessment," *Communications in Statistics – Theory and Methods*, vol. 9, no. 17, pp. 1749–1842, 1980. https://doi.org/10.1080/03610928008827996.

[44] Z. Kala, "Reliability of steel members designed in accordance with the code design concepts," *AIP Conference Proceedings*, vol. 1281, pp. 579–582, 2010. https://doi.org/10.1063/1.3498542.

**Contribution of individual authors to the creation of a scientific article (ghostwriting policy)**

Author Contributions: All the work was carried out solely by one author, at all stages from the formulation of the problem to the final findings and solution.

**Sources of funding for research presented in a scientific article or scientific article itself**

The sources of funding are from the project "Importance of Stochastic Interactions in Computational Models of Structural Mechanics" of The Czech Science Foundation (GACR, https://gacr.cz/), grant number 23-04712S, in Czechia.

**Conflict of Interest**

The author has no conflict of interest to declare that is relevant to the content of this article.